

## A new leaf phenology for the land surface scheme TERRA of the COSMO atmospheric model

JAN-PETER SCHULZ<sup>1,3,\*</sup>, GERD VOGEL<sup>2</sup>, AND BODO AHRENS<sup>3</sup>

<sup>1</sup>*LOEWE Biodiversity and Climate Research Centre, Senckenberganlage 25,  
D-60325 Frankfurt am Main, Germany*

<sup>2</sup>*Deutscher Wetterdienst, Meteorological Observatory Lindenberg – Richard-Aßmann-Observatory,  
D-15848 Tauche OT Lindenberg, Germany*

<sup>3</sup>*Goethe University Frankfurt, Institute for Atmospheric and Environmental Sciences,  
Altenhöferallee 1, D-60438 Frankfurt am Main, Germany*

*\*Corresponding author: Jan-Peter Schulz, affiliation now: Deutscher Wetterdienst,  
Frankfurter Straße 135, D-63067 Offenbach am Main, Germany*

### 1 Introduction

The terrestrial biosphere has a significant impact on near-surface atmospheric phenomena by modifying the energy and water balance at the land surface. In particular, it determines the evapotranspiration and therefore the latent and sensible heat fluxes over land, and thus can considerably affect atmosphere and land characteristics, such as near-surface temperature and humidity, low-level clouds and precipitation (Arora, 2002).

In soil-vegetation-atmosphere transfer (SVAT) schemes the role of vegetation in controlling the energy and water balance is considered by taking into account its physiological properties, in particular, leaf area index (LAI, the ratio of leaf to ground area), stomatal resistance, and rooting depth. However, many SVAT schemes do not describe the vegetation as a dynamic component. The seasonal evolution of its physiological properties is prescribed as a climatology, being the same for each year of a simulation (see e. g. ECMWF, 2014).

This is also the case for the SVAT scheme TERRA of the Consortium for Small-scale Modeling (COSMO) mesoscale atmospheric model (Steppeler et al., 2003). There are different options for specifying the seasonal cycle of the LAI. In one method, a minimum and a maximum value of the LAI are specified, depending on land use, representing vegetation at rest and during the growing season, and the seasonal cycle is prescribed by a sinusoidal fit for the transitions between these values in spring and autumn (Doms et al., 2011). This is currently the default in the COSMO model for numerical weather prediction (NWP). In another method, climatological monthly mean values of the LAI are specified which are based on satellite retrievals. A short-coming of these methods is that the model can not account for inter-annual variations of the seasonal evolution of the vegetation. In some years the spring and growing season start earlier, in some years they are delayed. In these cases, the state of the vegetation is not accurately represented in the model when prescribing the leaf phenology by a climatology, leading to errors in for instance the evapotranspiration.

In this study, two phenology models are presented, based on Polcher (1994) and on Knorr et al. (2010), which allow the vegetation in TERRA to adapt to the simulated seasonal and inter-annual variations in weather and climate, as well as to habitat factors, such as elevation.

### 2 Model description

The COSMO model (Steppeler et al., 2003; Doms et al., 2011) is a nonhydrostatic limited-area atmospheric prediction model, which is developed and maintained by the COSMO consortium (<http://www.cosmo-model.org>). It is designed for both operational numerical weather prediction and various scientific applications on the meso- $\beta$  and meso- $\gamma$  scale. Furthermore, the COSMO model was expanded by the CLM community (<http://www.clm-community.eu>) to become applicable as a regional climate model, called COSMO-CLM (e. g. Rockel et al., 2008).

A variety of physical processes is taken into account by parameterization schemes, including the soil and vegetation model TERRA (Doms et al., 2011). It simulates the energy and water balance at the land surface and in the ground, providing the land surface temperature and humidity as lower boundary conditions for

computing the energy and water fluxes between surface and atmosphere. In TERRA, all processes are modelled one-dimensionally in the vertical, no lateral interactions between adjacent soil columns are considered.

The soil temperature is calculated by the heat conduction equation, while the soil water content is predicted by the Richards equation. Both equations are discretized by a multi-layer scheme using the same layer depths for both temperature and water content. This allows to include the freezing and thawing of soil water or ice, respectively. At the interface between surface and atmosphere, the surface energy balance equation is solved, yielding the new surface temperature. It takes into account the total surface net radiation, the sensible and latent heat flux, and the ground heat flux. The atmospheric energy fluxes constitute the upper boundary condition of the soil heat conduction equation.

Precipitation reaching the ground is separated into infiltration or surface runoff. The simulation of the water vapour flux, returning moisture from the ground back to the atmosphere, depends on the land use. For vegetated areas, transpiration from the vegetation is computed, taking into account the plant physiological properties, and for non-vegetated areas, bare soil evaporation is computed. The total moisture flux, the evapotranspiration, at a grid element is calculated as an area weighted average of the individual fluxes. In the standard model configuration, the formulations of both components of the evapotranspiration are based on BATS (Dickinson, 1984). During this study, it turned out that the bare soil evaporation based on BATS is overestimated. Therefore, it was replaced by a formulation based on ISBA (Noilhan and Planton, 1989), yielding, for instance, a more realistic simulation of the annual cycle of soil moisture. The snow pack is simulated by a single-layer snow model, taking into account snow ageing with respect to albedo and density.

In TERRA, the vegetation is described basically by three parameters, i. e. the vegetation ratio (the fractional area of a grid element covered by vegetation), the LAI, and the rooting depth. The different options for specifying the seasonal cycle of the LAI and the vegetation ratio compared in this study are described in section 3. For the comparison, here the same exponential root profile is used for the different options, which is constant in time.

### 3 Seasonal cycle of the LAI

The parameter values describing the vegetation at a particular element of the model grid are determined by the dominant land use class as given by a land use dataset (Smiatek et al., 2008; Smiatek, 2014). In TERRA, the following parameters are needed: Minimum and maximum vegetation ratio ( $\sigma_{\min}$  and  $\sigma_{\max}$ ), representing vegetation at rest and during the growing season, minimum and maximum LAI ( $\text{LAI}_{\min}$  and  $\text{LAI}_{\max}$ ), and rooting depth.

#### 3.1 Current parameterization (sinusoidal fit)

In order to specify a seasonal cycle of the LAI and the vegetation ratio, in the currently used standard configuration of the COSMO model for NWP a simple empirical analytical function is prescribed to interpolate between their minimum and maximum values (Doms et al., 2011). This function depends on the latitude  $\varphi$  and the altitude of the location, and on the initial Julian day  $J_d$  of the forecast. It is computed by the preprocessing procedure INT2LM which provides the initial and boundary conditions for the model (Schättler, 2014).

The Julian day  $V_s$ , when the vegetation period starts, and its length  $V_i$  (in days) are estimated by the following formulae:

$$V_s = \max(1.0, 3.0(|\varphi| - 20^\circ)), \quad (1)$$

$$V_i = \min(365.0, 345.0 - 4.5(|\varphi| - 20^\circ)). \quad (2)$$

The following reduction factor  $f_h$  depending on surface geopotential height  $\Phi_S$  describes the effect of an increasing altitude:

$$f_h(\Phi_S) = e^{-5 \cdot 10^{-9} \cdot \Phi_S^2}. \quad (3)$$

The seasonal cycle of the LAI (and of the vegetation ratio in a similar way) is given by:

$$\text{LAI}(\varphi, \Phi_S, J_d) = \text{LAI}_{\min} + (\text{LAI}_{\max} - \text{LAI}_{\min}) \cdot f_v \cdot f_h(\Phi_S), \quad (4)$$

with

$$f_v = \max(0.0, \min(1.0, 1.12 \cdot \sin(\pi \cdot \max(0.0, (J_d - V_s)/V_l))))). \quad (5)$$

### 3.2 Dynamic phenology adapting to meteorological conditions

The phenology is mainly determined by three meteorological, or climatological, conditions: temperature, day length, and water availability. Whenever one or more of these factors are not sufficiently supplied, the vegetation will experience “stress”, limiting its ability to fully get developed. Beside these, there exist other limiting factors, for instance the net primary productivity (NPP), which is the result of photosynthetic activity and respiration of the vegetation and requires the treatment of CO<sub>2</sub> concentrations and fluxes in the atmospheric model (see e. g. Arora, 2002). There are several dynamic global vegetation models which make use of NPP dependent formulations of phenology, for instance, JSBACH (see e. g. Raddatz et al., 2007), CLM (Oleson et al., 2013), or ORCHIDEE (Krinner et al., 2005). But, since the COSMO atmospheric model does not include a carbon cycle we restrict ourselves to schemes without the need of NPP. Two phenology models are compared in this study, a diagnostic and a prognostic one, based on Polcher (1994) and on Knorr et al. (2010). They were both implemented in the TERRA offline model.

In order to describe the stress with respect to temperature, a phenology determining temperature  $T$  (based on Knorr et al., 2010) is defined by:

$$T(t) = \frac{\int_{-\infty}^0 T_S(t + \tilde{t}) e^{\frac{\tilde{t}}{\tau}} d\tilde{t}}{\int_{-\infty}^0 e^{\frac{\tilde{t}}{\tau}} d\tilde{t}}, \quad (6)$$

where  $\tau$  is the averaging period for the surface temperature  $T_S$ , and  $t$  is the time. This formula uses exponentially declining weights when going back into the past, which is equivalent to an exponentially declining memory of the plants for the surface temperature. The averaging period is chosen to be 15 days, this makes sure that the diurnal cycles and other short-term fluctuations of  $T_S$  are sufficiently dampened, while not making the evolution of  $T(t)$  too inert which would delay the vegetation period.

#### 3.2.1 Polcher (1994)

Here, a purely temperature-limited LAI is adopted in modified form from Polcher (1994):

$$\text{LAI}(t) = \begin{cases} \text{LAI}_{\min} & , \text{ if } T(t) \leq T_1, \\ \text{LAI}_{\min} + \frac{T(t) - T_1}{T_2 - T_1} (\text{LAI}_{\max} - \text{LAI}_{\min}) & , \text{ if } T_1 < T(t) \leq T_2, \\ \text{LAI}_{\max} & , \text{ if } T_2 < T(t), \end{cases} \quad (7)$$

where  $T_1$  is the minimum limiting temperature, and  $T_2$  the maximum limiting temperature. These two parameters depend on the phenology type.

#### 3.2.2 Knorr et al. (2010)

The phenology model by Knorr et al. (2010) includes limiting factors due to temperature, day length, and water availability. But, for the comparison with Polcher (1994), here the focus is set on the temperature, while excluding the day length and water limitations. This leads to:

$$\frac{d\text{LAI}(t)}{dt} = \begin{cases} k_{\text{grow}}(\text{LAI}_{\max} - \text{LAI}(t)), & \text{ if } T(t) \geq T_{\text{on/off}}, \\ k_{\text{shed}}(\text{LAI}_{\min} - \text{LAI}(t)), & \text{ else,} \end{cases} \quad (8)$$

where  $T_{\text{on/off}}$  is the leaf onset and offset temperature, and  $k_{\text{grow}}$  and  $k_{\text{shed}}$  are the growth rate and the shedding rate, respectively. These parameters depend on the phenology type.

## 4 Experiments and observational data

In order to compare the three phenology schemes described in section 3, experiments with the land surface scheme TERRA in offline mode were carried out. This methodology is described e. g. by Chen et al. (1997) or Schulz et al. (1998). For this comparison, TERRA was forced in each simulation with a set of identical atmospheric observations, which are downward shortwave and longwave radiation, total precipitation, near-surface wind speed, air temperature, and specific humidity. For this study, observations from the boundary layer field site Falkenberg were used, providing the atmospheric forcing variables as mentioned before, as well as several quantities for model validation, such as e. g. surface latent heat flux.

Falkenberg is a site at the Meteorological Observatory Lindenberg – Richard-Aßmann-Observatory – of the German Meteorological Service (Deutscher Wetterdienst), located about 5 km south of the observatory. It is a grass land site representative for farmland surfaces in the heterogeneous rural landscape typical for large parts of northern central Europe (Neisser et al., 2002; Beyrich et al., 2006). It is in continuous operation since 1998 with a main focus on the near-surface boundary layer and soil processes. A detailed description of the measurement conditions, instrumentation, data acquisition and the comprehensive quality control procedures is given by Beyrich and Adam (2007).

The offline simulations were carried out for five selected years between 2006 and 2013. They represent very different seasonal cycles in terms of temperature and precipitation. Some years had a very warm spring, e. g. 2007, and some years a cold one, e. g. 2013. It is expected that, in contrast to the current parameterization, the two temperature-dependent phenology schemes presented here will respond to these different seasonal cycles. A warm spring may lead to an early begin of vegetation activity, a cold one to a late begin. The main land surface parameter values needed to appropriately describe the Falkenberg site within TERRA are given in Table 1. They were based on measurements and estimates adapted to the site conditions. The predominant vegetation species are perennial ryegrass (*Lolium perenne*) and red fescue (*Festuca rubra*). For these grass species an albedo value of 0.18 was used. The soil texture especially prevailing at the radiation measurement spot is dominated by sandy pale soil (*Eutric Podzoluvisol*), (see Hierold, 1997) according to the FAO soil classification (FAO, 1988), for which an albedo value of 0.2 was used. The prescribed albedo values are in good agreement with experimental findings for this site described by Beyrich and Adam (2007). Although the meadow of the site is mowed several times a year to keep the vegetation height below 20 cm, the impact of the surrounding crop fields on the 10 m wind speed was represented by a slightly increased roughness length  $z_0$  of 0.03 m on annual average.

The additional parameter values needed for the phenology models by Polcher (1994) and Knorr et al. (2010) were estimated as follows:  $T_1 = 2^\circ\text{C}$ ,  $T_2 = 15^\circ\text{C}$ , and  $T_{\text{on/off}} = 5^\circ\text{C}$ ,  $k_{\text{grow}} = k_{\text{shed}} = 0.07 \text{ d}^{-1}$ .

Table 1: Main land surface parameter values in TERRA representing the Falkenberg site.  $\sigma_{\text{min}}$  and  $\sigma_{\text{max}}$  are the minimum and maximum vegetation ratio, representing grass at rest and during the growing season.  $\text{LAI}_{\text{min}}$  and  $\text{LAI}_{\text{max}}$  are the respective values but for the leaf area index.  $\alpha_{\text{gr}}$  and  $\alpha_{\text{bs}}$  are the surface albedos for grass and bare soil, and  $z_{0,\text{gr}}$  and  $z_{0,\text{bs}}$  are the turbulent roughness lengths for grass and bare soil, respectively.

Parameter	$\sigma_{\text{min}}$	$\sigma_{\text{max}}$	$\text{LAI}_{\text{min}}$	$\text{LAI}_{\text{max}}$	$\alpha_{\text{gr}}$	$\alpha_{\text{bs}}$	$z_{0,\text{gr}}$ (m)	$z_{0,\text{bs}}$ (m)
Value	0.55	0.80	0.5	2.5	0.18	0.20	0.03	0.03

## 5 Results

The phenology models adopted from Polcher (1994) and Knorr et al. (2010) are compared to the current parameterization of the LAI, using the land surface scheme TERRA in offline mode by applying the methodology as described in section 4. Figure 1 illustrates the annual cycles of the 2-m temperature as measured at Falkenberg during the years 2006, 2007, 2008, 2012, and 2013. They show a considerable inter-annual variability. Some years have a very warm spring, e. g. 2007, and some years have a cold one, e. g. 2013. In autumn, the differences are smaller, but there are also warm years, e. g. 2006, and cold years, e. g. 2007.

When running the land surface scheme TERRA in offline mode, using the phenology model based on Polcher (1994), it results in five different annual evolutions of the LAI. As shown in Fig. 2 a warm spring such as in 2007 leads to an early rise of the LAI, or an early begin of vegetation activity, and a cold spring such as in 2013 results in a late rise of the LAI. A warm autumn, on the other hand, leads to a late decline of the LAI, e. g. in 2006, and a cold autumn results in an early drop of the LAI, e. g. in 2007. This means that the phenology model allows the vegetation in TERRA to adapt to the simulated seasonal and inter-annual

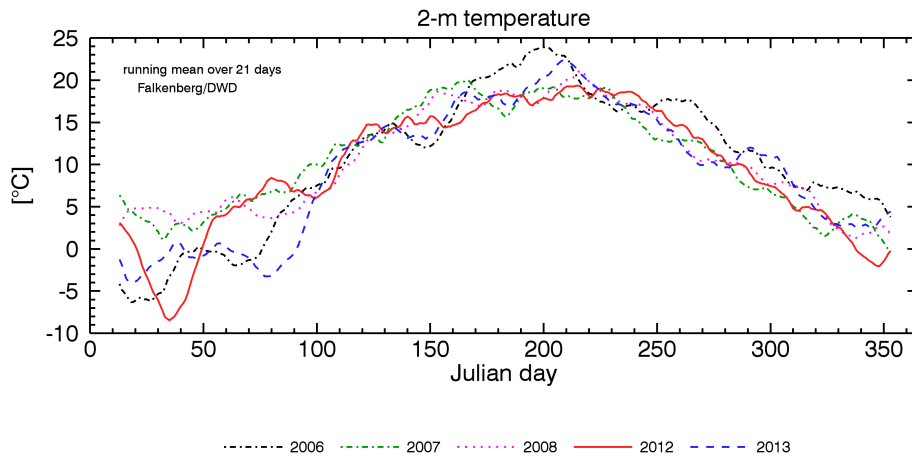


Figure 1: Annual cycles of the 2-m temperature as measured at Falkenberg during the years 2006, 2007, 2008, 2012, and 2013. A running mean over 21 days was applied to the data.

variations in weather and climate. This is a clear improvement compared to the sinusoidal fit of the current parameterization, shown in Fig. 2 for reference, which can not account for this variability.

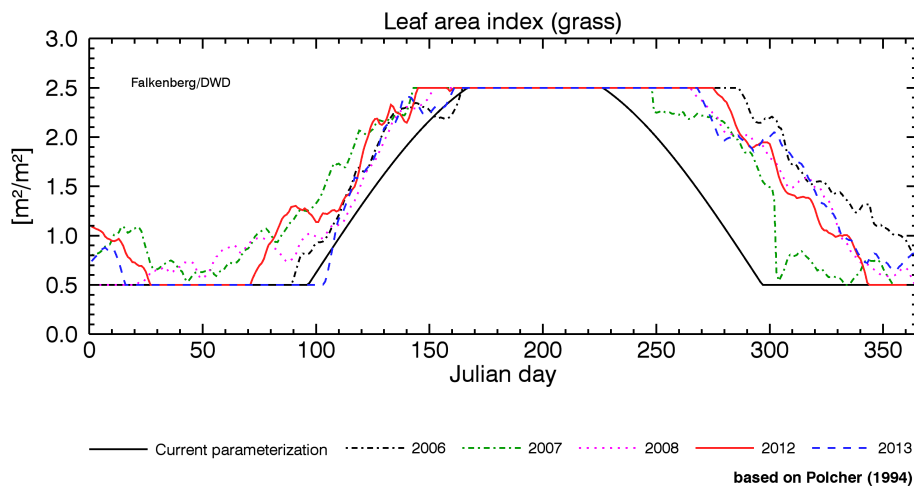


Figure 2: Annual cycles of the LAI at Falkenberg during the years 2006, 2007, 2008, 2012, and 2013 based on Polcher (1994). For comparison, the sinusoidal fit of the current parameterization is shown.

A shortcoming of a diagnostic model such as the one by Polcher (1994) may be that the LAI has to always closely follow the evolution of the driving quantities, here the temperature. This can lead to a drop of the LAI during its rising phase in spring which may not be realistic for many species. In contrast, in a prognostic model such as the one by Knorr et al. (2010), the LAI will keep on rising once the trigger for leaf onset is set. The underlying concept is that the initial leaf development relies on the buds and the reserves from the previous year. Leaf unfolding and growth will continue even if the surface stays cool for a while, as long as it does not return to frost or winter conditions.

The result is shown in Fig. 3. Once the leaf onset temperature is exceeded in spring, leaf unfolding and growth start, and the LAI starts rising asymptotically towards its maximum value. In autumn, this works in opposite direction. The order of the years is almost similar in Figs. 2 and 3. The warm spring in 2007 leads to an early rise of the LAI also for the phenology model based on Knorr et al. (2010), and the cold spring in 2013 results in a late rise of the LAI. A similar order of the years is also found in autumn, for instance, for the early

dropping LAI in 2007 and the lately declining LAI in 2006. An exception is the year 2008 in which the LAI starts rising much earlier based on Knorr et al. (2010) than based on Polcher (1994). This shows the need for a careful calibration of the various threshold values, for instance for temperature, for the different phenology types.

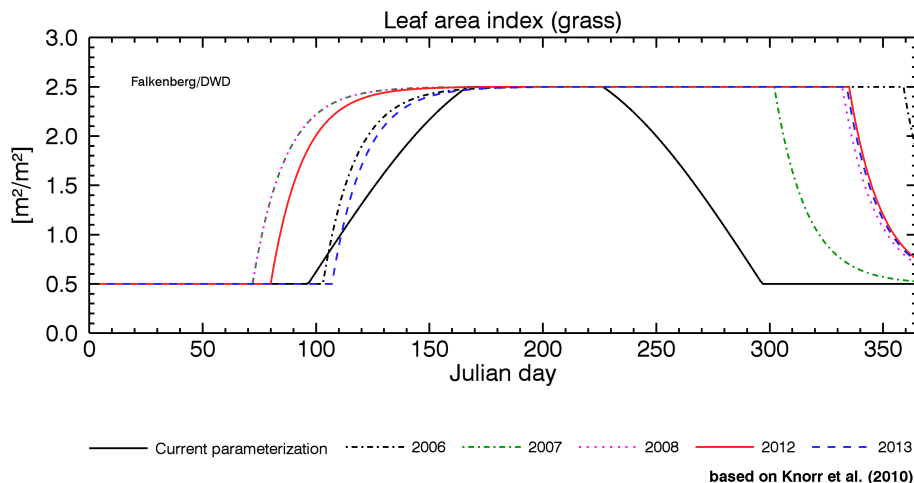


Figure 3: Same as Fig. 2 but for Knorr et al. (2010).

Due to the lack of in-situ observations of the LAI at Falkenberg, here an attempt for an indirect validation of the different models is made, using measurements of the surface latent heat flux at Falkenberg. Figure 4 compares the diurnal cycles of the observed and the simulated latent heat fluxes, averaged over the spring period of 1–20 April 2007 (Julian day 91–110). During this period, the LAI of the current parameterization increases from 0.5 to about 1.0, the LAI based on Polcher (1994) rises within the range of about 1.2 to 1.8 (both see Fig. 2), and the LAI based on Knorr et al. (2010) is already in the range of about 2.0 to 2.3 (see Fig. 3). As a consequence of these differences in LAI based on the three phenology models compared here, the transpiration and therefore the latent heat flux as simulated by TERRA show distinct differences as well. As depicted by Fig. 4, the maximum of the latent heat flux as simulated by the current parameterization is at about  $90 \text{ W/m}^2$ , which is clearly underestimating the measurement, the maximum based on Polcher (1994) is increased to about  $120 \text{ W/m}^2$ , while the one based on Knorr et al. (2010) reaches about  $150 \text{ W/m}^2$ . The latter is very similar to the measurement. These results suggest that the current parameterization of the LAI is not able to accurately describe its early rise during the warm spring of 2007, while the two temperature-dependent phenology models based on Polcher (1994) and on Knorr et al. (2010) provide an earlier and more realistic increase of the LAI.

Qualitatively similar results are found for a period of leaf shedding in the autumn of 2007, as illustrated in Fig. 5.

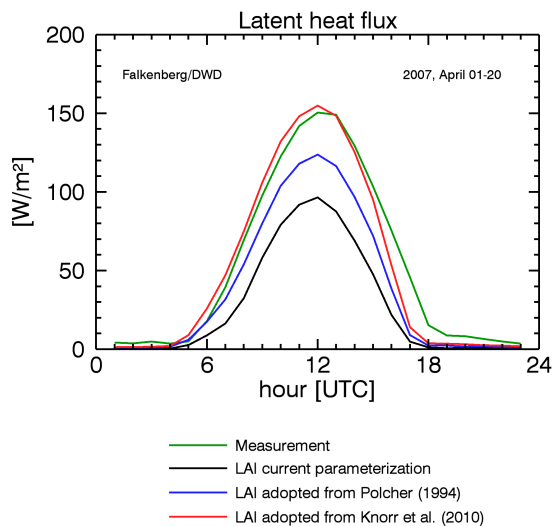


Figure 4: Mean diurnal cycles of the surface latent heat flux as measured at Falkenberg on 1–20 April 2007 (Julian day 91–110) compared to the results of the current parameterization of the LAI, and the results based on Polcher (1994) and on Knorr et al. (2010).

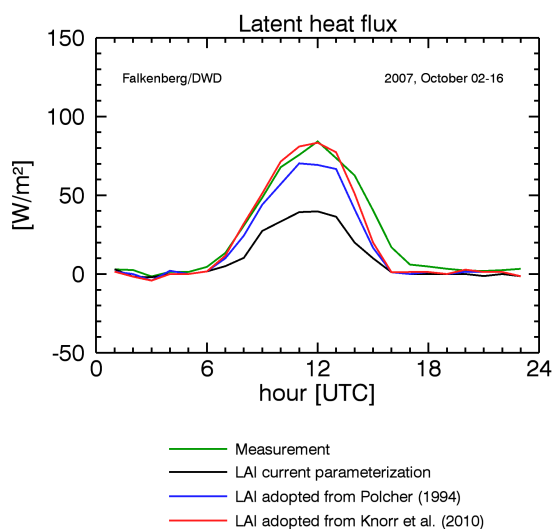


Figure 5: Same as Fig. 4 but for 2–16 October 2007 (Julian day 275–289).

## 6 Conclusions

Two temperature-dependent phenology models based on Polcher (1994) and on Knorr et al. (2010) were compared to the current parameterization of the LAI as used in the land surface scheme TERRA of the COSMO atmospheric model.

Currently, in TERRA a minimum and a maximum value of the LAI are specified, depending on land use, representing vegetation at rest and during the growing season, and the seasonal cycle of the LAI is prescribed by a sinusoidal fit for the transitions between these values in spring and autumn. As a consequence, the model can not account for inter-annual variations of the seasonal evolution of the vegetation, leading to errors in for instance the evapotranspiration.

The two modified versions of TERRA, including the phenology models based on Polcher (1994) and on Knorr et al. (2010), allow the vegetation in TERRA to adapt to the simulated seasonal and inter-annual variations in weather and climate, as well as to habitat factors, such as elevation. Polcher (1994) uses a diagnostic approach, directly relating the LAI to temperature, while Knorr et al. (2010) follow a prognostic approach, utilizing the concept of growth and shedding rates. The latter appears to be generally favourable.

Experiments with TERRA in offline mode, using observations from the boundary layer field site Falkenberg, have shown that the current parameterization of the LAI tends to significantly underestimate the surface latent heat flux during the transition periods in spring and autumn. In the case of the year 2007, this behaviour was found to be substantially improved by the model based on Polcher (1994). Furthermore, the simulated diurnal cycles of latent heat flux based on Knorr et al. (2010) were found to be very close to the observations, in terms of amplitude as well as phase.

This study was restricted to the temperature limitation of the LAI. The next step will be the extension of the phenology model to the limiting factors due to day length and water availability. This is already prepared in the work by Knorr et al. (2010). Furthermore, for global applicability, an extension to more phenology types, beside grass, is needed, for instance shrubs and trees (deciduous and evergreen). Finally, the phenology model needs to be transferred and implemented into the three-dimensional coupled COSMO model code.

## Acknowledgements

The authors thank Udo Rummel, Deutscher Wetterdienst, for his assistance with the Lindenberg observational data. We further acknowledge funding from the Hessian initiative for the development of scientific and economic excellence (LOEWE) at the Biodiversity and Climate Research Centre (BiK-F), Frankfurt am Main. This work was supported by the German Federal Ministry of Education and Research (BMBF) under grant MiKliP: DECRET/01LP1118B, DEPARTURE/01LP1129D.

## References

- [1] Arora, V., 2002: Modeling vegetation as a dynamic component in soil-vegetation-atmosphere transfer schemes and hydrological models. *Rev. Geophys.*, **40**(2), 1006, doi:10.1029/2001RG000103, 26 pp.
- [2] Beyrich, F., and W. K. Adam, 2007: Site and data report for the Lindenberg reference site in CEOP – Phase 1. *Berichte des Deutschen Wetterdienstes*, No. 230, Offenbach am Main, 55 pp. ISBN/EAN:978-3-88148-422-0.
- [3] Beyrich, F. (Ed.), S. H. Richter, U. Rummel, and U. Weisensee, 2006: Ausgewählte Ergebnisse von Bodenfeuchtemessungen am Meteorologischen Observatorium Lindenberg. *Deutscher Wetterdienst – Forschung und Entwicklung*, Arbeitsergebnisse Nr. 84, Offenbach am Main, 46 pp. ISSN 1430-0281.
- [4] Chen, T. H., A. Henderson-Sellers, P. C. D. Milly, A. J. Pitman, A. C. M. Beljaars, J. Polcher, F. Abramopoulos, A. Boone, S. Chang, F. Chen, Y. Dai, C. E. Desborough, R. E. Dickinson, L. Dümenil, M. Ek, J. R. Garratt, N. Gedney, Y. M. Gusev, J. Kim, R. Koster, E. A. Kowalczyk, K. Laval, J. Lean, D. Lettenmaier, X. Liang, J.-F. Mahfouf, H.-T. Mengelkamp, K. Mitchell, O. N. Nasonova, J. Noilhan, A. Robock, C. Rosenzweig, J. Schaake, C. A. Schlosser, J.-P. Schulz, Y. Shao, A. B. Shmakin, D. L. Verseghy, P. Wetzell, E. F. Wood, Y. Xue, Z.-L. Yang, and Q. Zeng, 1997: Cabauw experimental results from the Project for Intercomparison of Land-surface Parameterization Schemes. *J. Climate*, **10**, 1194–1215.
- [5] Dickinson, R. E., 1984: Modeling evapotranspiration for three-dimensional global climate models: Climate processes and climate sensitivity. *Geophys. Monogr.*, **29**, Maurice Ewing Volume 5, 5, 58–72.



- [6] Doms, G., J. Förstner, E. Heise, H.-J. Herzog, D. Mironov, M. Raschendorfer, T. Reinhardt, B. Ritter, R. Schrodin, J.-P. Schulz, and G. Vogel, 2011: A description of the nonhydrostatic regional COSMO model. Part II: Physical parameterization. *Deutscher Wetterdienst*, Offenbach, 154 pp. (Available at <http://www.cosmo-model.org/>).
- [7] ECMWF, 2014: IFS documentation – Cy40r1. Part IV: Physical processes. *European Centre for Medium-Range Weather Forecasts*, Reading, 190 pp. (Available at <http://www.ecmwf.int/>).
- [8] FAO, 1988: Soil map of the world. *Food and Agriculture Organization of the United Nations*, Rome, 119 pp.
- [9] Hierold, W., U. Schumacher, R. Ziethen, and D. Becker, 1997: Kartierbericht. Ergebnisse der bodenkundlichen Kartierung zum Messfeld Falkenberg des Meteorologischen Observatoriums Lindenberg des DWD. *Deutscher Wetterdienst*, Internal report, Lindenberg, 26 pp.
- [10] Knorr, W., T. Kaminski, M. Scholze, N. Gobron, B. Pinty, R. Giering, and P.-P. Mathieu, 2010: Carbon cycle data assimilation with a generic phenology model. *J. Geophys. Res.*, **115**, G04017, doi:10.1029/2009JG001119, 16 pp.
- [11] Krinner, G., N. Viovy, N. de Noblet-Ducoudré, J. Ogée, J. Polcher, P. Friedlingstein, P. Ciais, S. Sitch, and I. C. Prentice, 2005: A dynamic global vegetation model for studies of the coupled atmosphere-biosphere system. *Global Biogeochem. Cycles*, **19**, GB1015, doi:10.1029/2003GB002199, 33 pp.
- [12] Neisser, J., W. Adam, F. Beyrich, U. Leiterer, and H. Steinhagen, 2002: Atmospheric boundary layer monitoring at the Meteorological Observatory Lindenberg as a part of the “Lindenberg Column”: Facilities and selected results. *Meteor. Z.*, **11**, 241–253.
- [13] Noilhan, J., and S. Planton, 1989: A simple parameterization of land surface processes for meteorological models. *Mon. Wea. Rev.*, **117**, 536–549.
- [14] Oleson, K. W., D. M. Lawrence, G. B. Bonan, B. Drewniak, M. Huang, C. D. Koven, S. Levis, F. Li, W. J. Riley, Z. M. Subin, S. C. Swenson, P. E. Thornton, A. Bozbiyik, R. Fisher, C. L. Heald, E. Kluzek, J.-F. Lamarque, P. J. Lawrence, L. R. Leung, W. Lipscomb, S. Muszala, D. M. Ricciuto, W. Sacks, Y. Sun, J. Tang, and Z.-L. Yang, 2013: Technical description of version 4.5 of the Community Land Model (CLM). *National Center for Atmospheric Research*, Technical Note NCAR/TN-503+STR, Boulder, CO, 420 pp.
- [15] Polcher, J., 1994: *Etude de la sensibilité du climat tropical à la déforestation*. Thèse de doctorat, Univ. Pierre et Marie Curie, Paris.
- [16] Raddatz, T. J., C. H. Reick, W. Knorr, J. Kattge, E. Roeckner, R. Schnur, K.-G. Schnitzler, P. Wetzel, and J. Jungclaus, 2007: Will the tropical land biosphere dominate the climate-carbon cycle feedback during the 21st century?. *Climate Dyn.*, **29**, 565–574.
- [17] Rockel, B., A. Will, and A. Hense, 2008: The regional climate model COSMO-CLM (CCLM). *Meteor. Z.*, **17**, 347–348.
- [18] Schättler, U., 2014: A description of the nonhydrostatic regional COSMO model. Part V: Preprocessing: Initial and boundary data for the COSMO model. *Deutscher Wetterdienst*, Offenbach, 74 pp. (Available at <http://www.cosmo-model.org/>).
- [19] Schulz, J.-P., L. Dümenil, J. Polcher, C. A. Schlosser, and Y. Xue, 1998: Land surface energy and moisture fluxes: Comparing three models. *J. Appl. Meteor.*, **37**, 288–307.
- [20] Smiatek, G., 2014: Time invariant boundary data of regional climate models COSMO-CLM and WRF and their application in COSMO-CLM. *J. Geophys. Res. Atmos.*, **119**, 7332–7347.
- [21] Smiatek, G., B. Rockel, and U. Schättler, 2008: Time invariant data preprocessor for the climate version of the COSMO model (COSMO-CLM). *Meteor. Z.*, **17**, 395–405.
- [22] Steppeler, J., G. Doms, U. Schättler, H.-W. Bitzer, A. Gassmann, and U. Damrath, 2003: Meso-gamma scale forecasts using the nonhydrostatic model LM. *Meteor. Atmos. Phys.*, **82**, 75–96.